

Knockdown of miR-23, miR-27, and miR-24 Alters Fetal Liver Development and Blocks Fibrosis in Mice

Charles E. Rogler, Joe S. Matarlo, Brian Kosmyrna, Daniel Fulop, and Leslie E. Rogler

Division of Gastroenterology and Liver Disease, Department of Medicine, Marion Bessin Liver Research Center, Albert Einstein College of Medicine, Bronx, NY, USA

MicroRNAs (miRNAs) regulate cell fate selection and cellular differentiation. miRNAs of the miR23b polycistron (miR-23b, miR-27b, and miR-24) target components of the TGF- β signaling pathway and affect murine bile ductular and hepatocyte cell fate selection in vitro. Here we show that miR-23b polycistron miRNAs directly target murine Smad4, which is required for TGF- β signaling. Injection of antagomirs against these miRNAs directly into E16.5 murine fetuses caused increased cytokeratin expression in sinusoids and primitive ductular elements throughout the parenchyma of newborn mice. Similar antagomir injection in newborn mice increased bile ductular differentiation in the liver periphery and reduced hepatocyte proliferation. Antagomir injection in newborn Alb/TGF- β 1 transgenic mice that develop fibrosis inhibited the development of fibrosis, and injection of older mice caused the resolution of existing fibrosis. Furthermore, murine stellate cell activation, including ColA1 and ACTA2 expression, is regulated by miR-23b cluster miRNAs. In summary, knockdown of miR-23b cluster miRNAs in fetal and newborn liver promotes bile duct differentiation and can block or revert TGF- β -induced liver fibrosis that is dependent on stellate cell activation. These data may find practical application in the highly needed development of therapies for the treatment of fibrosis.

Key words: Alb/TGF- β 1; MicroRNA; miR-23; miR-27; miR-24; Liver; Liver fibrosis; Cell fate; Differentiation; Hepatic progenitors

INTRODUCTION

MicroRNAs (miRNAs) are small, noncoding RNAs, 21 to 23 nucleotides in length, that regulate gene expression¹. The impact of miRNAs on gene expression is dependent on multiple factors including the relative abundance of miRNA and target transcripts within the cell and the presence of RNA-binding proteins that interact with the miRNA binding site on the target transcript^{2–4}. The effect of miRNAs on target gene expression is not generally as an on–off switch, but rather as a molecular rheostat that fine-tunes cellular responses to gradients of growth factors and morphogens in developing systems and in cell fate selection^{5,6}. Therefore, experimental approaches treating tissues with anti-miRs and antagomirs necessarily will have cell type-dependent effects among the multiple differentiating cell types present in the treated tissues.

In the murine liver, the period between 15 days of gestation and birth is a period of massive cell growth and cell fate determination, particularly focused on establishment of hepatocyte parenchyma and early biliary components of the liver⁷. The process of cell fate selection begins near the hilum of the liver and continues

postnatally at the periphery⁷. At present, the molecular controls of the maturation of liver structure are poorly understood. Previous studies both in vitro and in vivo have supported a promotive role of transforming growth factor- β (TGF- β) in ductular development and the control of hepatocyte proliferation^{8–10}. Using a murine bipotent fetal liver cell line, HBC3, we showed that inhibition of TGF- β signaling by Smad4 knockdown blocked ductular morphogenesis, suggesting that TGF- β signaling promotes the formation of ductular structures in vitro. We showed that the response of these progenitor cells to TGF- β is modulated by the presence of miRNAs from the miR23b polycistron (miR-23b, miR-27b, and miR-24-1) that potentially targets transcripts encoding TGF- β receptors and intermediate signaling molecules including Smad3, Smad4, and Smad5⁴. These miRNAs are among the most highly expressed miRNAs in the fetal murine liver. They are expressed primarily in hepatoblasts undergoing hepatocytic differentiation but are low in cholangiocyte precursors⁴. This led us to hypothesize that the miRNAs miR-23, miR-27, and miR-24 act coordinately to influence cell fate selection (hepatocyte vs. cholangiocyte) in the developing murine liver.

In addition to its role in the establishment of the major epithelial cell types in the liver, TGF- β also plays an important role in the liver's response to injury^{11,12}. A common early feature of all chronic liver disease is deposition of extracellular matrix, whose source is myofibroblasts^{11,12}. The major source of myofibroblasts is the hepatic stellate cells (HSCs)¹³, although portal fibroblasts also contribute to fibrogenic myofibroblasts in response to cholestatic injury^{14,15}. Quiescent HSCs are located in the perisinusoidal space of Disse¹⁶. Morphologically, the cells are readily identifiable because of their stellate geometry and by the presence of prominent vitamin A-containing lipid droplets within their cytoplasm¹⁷⁻¹⁹. In addition, HSCs are the source of hepatocyte growth factor (HGF) within the liver^{20,21}. When HSCs are activated, they change morphology to become spindle shaped and proliferate²². This change is accompanied by a loss of vitamin A and down-regulation of neural markers and the acquisition of mesenchymal markers such as collagen α 1, α smooth muscle actin, and fibronectin^{16,23}. These cells become contractile and motile and migrate to the sites of injury²⁴.

One of the most important mediators of HSC activation is TGF- β ^{25,26}. The TGF- β signaling is mediated by the dimerization of the TGF- β receptor in response to binding by TGF- β ^{27,28}. The dimerized receptor phosphorylates the receptor Smads (Smad2 and Smad3)^{29,30}. The phosphorylated receptor Smads are released into the cytoplasm where they can bind Smad4³¹. This complex translocates into the nucleus where it regulates fibrogenic gene expression^{32,33}.

In this report, we have hypothesized that specific inhibition of highly expressed miRNAs from the miR-23b polycistron (miR-23b, miR-27b, and miR-24-1) would alter the cellular response to TGF- β superfamily signaling in vivo. We reasoned that the late fetal murine liver was an excellent organ in which to test the role of miRNAs in cell fate selection in late-stage development from E16.5 until birth. Specifically, we have developed a method to directly deliver anti-miRs to developing fetuses in utero at E16.5 and assay the effects of the treatments at E19.5, just prior to birth. We also expanded our investigations to include injection of neonatal Alb/TGF- β transgenic mice with the same anti-miRs to test their effect on TGF- β -induced liver fibrosis. The injection of antagomirs exposed a wide range of differentiating cell types to the anti-miRs and, dependent on the status of the endogenous miR-23 miRNAs, could produce cell type-dependent responses.

MATERIALS AND METHODS

Cell Culture

Hepal cells were cultured in Dulbecco's modified Eagle's medium (DMEM) high-glucose media (11965-118;

Life Technologies) supplemented with 10% fetal bovine serum and 1% penicillin-streptomycin and incubated at 37°C in a humidified 5% CO₂ in air atmosphere. LX2 cells were a gift of Dr. Scott Friedman. The cells were cultured as previously described³⁴.

Mutagenesis of 3'-UTR miRNA Binding Sites and Luciferase Assay

Putative binding sites for miR-23b, miR-27b, and miR-24 were identified using the RNAHybrid³⁵. Oligonucleotides were designed to introduce mutations in the sequences complementary to the miRNA seed site so that base pairing within positions 2 and 3 or 2 and 4 of the seed site would be disrupted. All mutations were introduced into PsiCheck2 plasmids containing wild-type 3'-UTR regions from Smad4 using Stratagene QuikChange Site-Directed Mutagenesis Kit according to the manufacturer's protocol as previously described⁴. The specific mutations introduced are described in Figure 1. Dual luciferase assays were performed as previously described⁴.

Protein Isolation and Western Blot Analysis

Hepal cells transfected with full-length Smad4 cDNA with either wild-type or mutated 3'-UTR sequence were washed with ice-cold Dulbecco's PBSA, scraped from the plate and pelleted by centrifuging at 100 \times g. The PBSA was aspirated, and 100 μ l of lysis buffer [20 mM Tris (pH 7.5), 150 mM NaCl, 1 mM EDTA, 1 mM EGTA, 1% Triton X-100, 2 mM β -glycerophosphate, 5 mM sodium phosphate, 2 mM sodium vanadate, 4 μ g/ml leupeptin, 8 μ g/ml pepstatin, and 1 mM PMSF] was added to the pellet and mixed by trituration. Samples were incubated at 4°C with rotation for 10 min, sonicated, aliquoted, and stored at -80°C. Protein concentration was measured using the Bio-Rad DC protein assay. Immunodetection of Smad4 protein was performed as previously described¹⁰.

Animal Maintenance

All animals were maintained in an ALLAC-approved animal facility at Albert Einstein College of Medicine. All procedures were carried out according to protocols approved by the Albert Einstein College of Medicine Institutional Animal Care and Use Committee. Swiss Webster outbred mice were used for antagomir injections as described below. Alb/TGF- β 1 transgenic mice in a C57/B16 genetic background³⁵ were obtained from the S. Thorgeirsson laboratory³⁵. The transgene in Alb/TGF- β 1 mice is located on the Y chromosome and is expressed through the albumin promoter nearly exclusively in the liver. This enabled us to use female littermates as control animals, based on the understanding that TGF- β 1 regulation of liver cell differentiation and endogenous miRNA expression are similar in males and females.

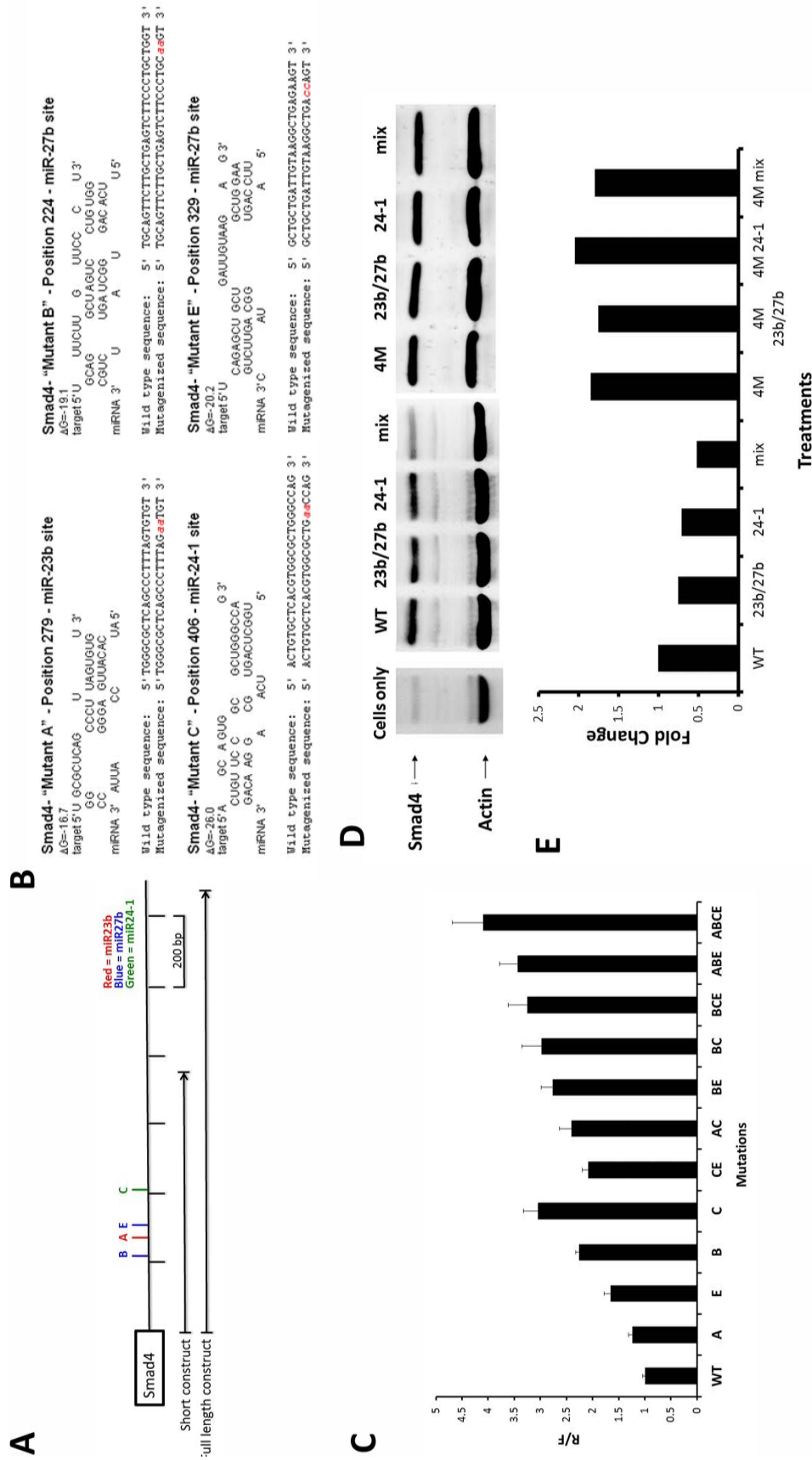


Figure 1. (A) Relative position map of miR-23b cluster validated target seed sites within the 3'-UTRs of Smad4. Red, blue, and green bars are validated functional target site positions for miR-23b, miR-27b, and miR-24-1, respectively. Black arrow bars represent segment length of the 3'-UTR constructs that were subcloned into PsiCheck2 dual luciferase vector (short and full) and pCMV.SPORT6.1 expression vector (full only). (B) Name and nucleotide position of seed sites on Smad4 3'-UTR. Target and miRNA sequence and theoretical interaction are shown. Mutation made in 3'-UTR is shown in red. (C) Hepa1 mouse cell line transfected with WT or mutagenized Smad4 3'-UTR panel. Results were normalized to WT baseline response to determine Renilla-to-Firefly fold change ratio. Four-mutant construct shows the most significant fold change, indicating the additive effect of blocking all seed sites corresponding to miR-23b, miR-27b, and miR-24-1. (D) Western blot analysis of Hepa1 cells transfected with only wild-type Smad4 (WT) or only Smad4 quadruple mutant (4M) expression constructs. Lentivirus expression mimics were cotransfected in the following combinations: 23b plus 27b, or 24-1 only, or a combination of all three. (E) Quantitative analysis of bands from the Western blot in (A). Densitometric analysis of Smad4 bands was normalized to actin as an internal loading control. These values were normalized to the WT baseline.

Antagomir Injection

Single Injections. Postnatal day 1 animals were injected intraperitoneally (IP) with 20 μ l of a solution of antagomirs in phosphate-buffered saline (PBS) at a dose of 45 mg/kg. Injections were made using a 30-gauge needle.

Multiple Injections. Animals were injected on postnatal days 1 and 7 at a dose of 45 mg/kg.

In Utero Injections. In utero injections were done at 16.5 days of gestation. Pregnant female mice were anesthetized using isoflourane gas. A flank incision of approximately 1 cm was made, and the uterine horns were exteriorized. Embryos in both uterine horns of pregnant females at E16.5 were injected using sterile technique. The embryos were injected through the uterine wall into the fetal peritoneum (IP) with 10 μ l of an antagomir mix against miR-23b cluster miRNAs at a dose of 20 mg/kg per fetus (E16.5 fetus is approximately 0.4 g). The dark liver of the embryos was used as a guide for injection. Embryos were harvested at E21 or birth. The sequence and modification of the antagomirs and mm-antagomirs were as follows: antagomir-23b, 5'-mG*mG*mUmAmAmUmCmCmCmUmGmGmCmAmAmUmGmU*mG*mA*mU*-3'-Chol; mm-antagomir-23b, 5'-mG*mG*mUmCmAmUmCmUmCmUmGmGmUmAmAmCmGmU*mG*mA*mU*-3'-Chol; antagomir-27b, 5'-mG*mC*mAmGmAmAmCmUmUmAmGmCmCmAmCmUmGmU*mG*mA*mA*-3'-Chol; mm-antagomir-27b, 5'-mG*mC*mAmGmCmAmCmUmCmAmGmCmUmAmCmUmAmU*mG*mA*mA*-3'-Chol; antagomir-24-1, 5'-mC*mU*mGmUmUmCmCmUmGmCmUmGmAmAmCmUmGmAmG*mC*mC*mA*-3'-Chol; mm-antagomir-24-1, 5'-mC*mU*mGmCmUmCmCmCmGmCmUmGmAmCmCmUmCmG*mC*mC*mA*-3'-Chol.

BrdU Injections

Mice (2 to 4 weeks old) were injected IP with 100 μ l of BrdU (10 μ g/ml) in Dulbecco's PBS 1 h prior to sacrifice. Tissues were formalin fixed and paraffin embedded. BrdU detection was performed using the BrdU Immunohistochemistry Kit (Cat. No. Ab125306; Abcam) following the manufacturer's protocol.

Histology

Routine histological staining for reticulin, Sirius Red, Ki-67, and cytokeratins was performed by the histology core of the Albert Einstein Analytical Ultrastructure Core. Cytokeratins were detected using a Pan CK antibody (mab1612; Chemicon Int.).

RNA isolation and qRT-PCR for miRNAs were performed as previously described⁴. Statistical analysis of qRT-PCR was carried using the Student's *t*-test as employed in Microsoft Excel.

Isolation of Mouse Hepatic Stellate Cells

Mouse HSCs were isolated from 10- to 14-week-old C57Bl6XDBA female mice as described by Mederacke et al.²². Following isolation, the cells were plated on Falcon 2003 tissue culture plates in DMEM high glucose, no pyruvate and supplemented with 10% fetal calf serum and 1% penicillin-streptomycin.

Transfection of miR-Zip or Lenti-miR Plasmids for miR-23b, miR-27b, and miR-24

miR-Zip and Lenti-miR plasmids were obtained from System Biosciences Inc. LX2 cells were plated at approximately 80% confluence in serum-containing medium without antibiotics. Prior to transfection, this medium was aspirated and replaced with serum-free media. Twenty-four micrograms of each plasmid, either alone or in combinations described in the text, was transfected using Lipofectamine 2000 (Life Technologies) according to the manufacturer's protocol. Cells were cultured for 48 h, and total RNA and small RNA preparations were prepared using RNeasy (Qiagen) and Ambion small RNA kits, respectively.

RESULTS

miR-23b Polycistron miRNAs Directly Target Smad4

In previous work, we showed that mimics of the miR-23b cluster miRNAs (miR-23b, miR-27b, and miR-24-1) block TGF- β -dependent ductular differentiation of murine fetal liver hepatoblasts⁴. Here we investigate the mechanism of this effect by mapping and validating miRNA target sites in the 3'-UTR of the key TGF- β signal transduction molecule, Smad4. We subcloned both a short and a full segment of the 3'-UTR into the PsiCheck2 reporter vector and created individual and combined mutants of the candidate target seed sites as shown (Fig. 1A). We identified four miRNA target sites in the Smad4 3'-UTR (Fig. 1B), one for miR-23b (Fig. 1B, position A), two for miR-27b (Fig. 1B, positions B and E), and one for miR-24 (Fig. 1B, position C). Other predicted target sites that were made and assayed did not show active miRNA regulation (data not shown).

Using murine Hepal cells, we assayed the effect of mutating the individual and combined seed sites on the derepression of *Renilla* reporter gene expression from the PsiCheck2 vector. Figure 1C shows significant derepression of *Renilla* signal caused by individual (A, B, C, and E) mutation of the candidate sites. More significantly, we also observed additive derepression when multiple sites were mutated in a single construct. The highest observed derepression was when all four candidate sites were mutated, strongly suggesting that all three of the miRNAs function cooperatively in posttranscriptional regulation of Smad4.

Next, we tested the effect of the four seed site mutations on Smad4 protein expression by transfecting a Smad4 expression vector containing either the wild-type (WT) 3'-UTR or the 3'-UTR containing all four mutant target sites (4M) into Hepa1 cells that normally contain a low Smad4 protein level. The results show that the construct containing the WT 3'-UTR expressed Smad4 normally, but cotransfection of miR-23b, miR-27b, and miR-24 mixture mimics caused a significant reduction of Smad4 expression (Fig. 1D and E). In contrast, the 4M construct had twofold more Smad4 expression with no significant change in expression level when cotransfected with the mixture of miRNA mimics (Fig. 1D and E).

Taken together, these data demonstrate the direct regulation of Smad4 by all three of the miR-23b polycistron miRNAs in vitro, and mutation of the four putative seed sites reduces the ability of these miRNAs to regulate Smad4 expression.

Knockdown of miR-23b Polycistron miRNAs in Fetal Liver Promotes Ductular Differentiation

The knockdown of miR-23b polycistron miRNAs promotes TGF- β signaling and promotes bile ductular differentiation of cultured murine hepatoblasts⁴. The E16.5 murine liver contains a dynamic mix of fetal liver stem cells that are in many different stages of hepatocytic or

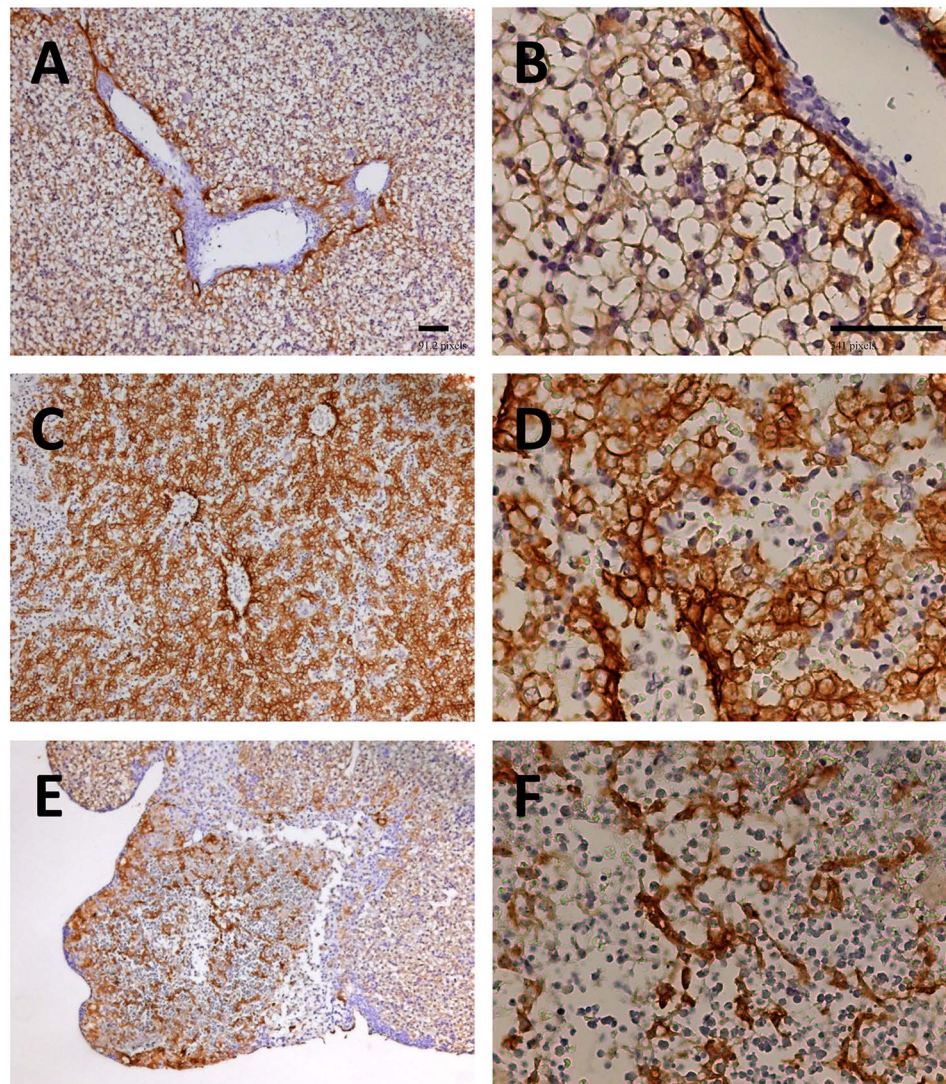


Figure 2. Effects of injection of murine E16.5 fetuses with miR-23b, miR-24-1, and miR-27b antagomir mix on the development of bile ducts in the liver at birth. (A) Low and (B) high magnification of cytokeratin staining marking bile ducts of control, PBS-injected fetal liver assayed at birth. (C, E) Low and (D, F) high magnification of cytokeratin staining of fetal livers injected with antagomir mix against miR-23b, miR-24-1, and miR-27b. Cytokeratin staining detected by brown staining. Scale bars: 100 μ m.

Table 1. Postnatal Knockdown of miR-23b, miR-27b, and miR-24 by Antagomir Treatment

Treatments	miR-23b	miR-27b	miR-24-1
P2	1 ± 0.01	1 ± 0.01	1 ± 0.01
P2 M antagomir	ND	0.09 ± 0.18	0.77 ± 0.02
P2 F antagomir	0.02 ± 0.005	0.13 ± 0.03	0.36 ± 0.01
P3 M antagomir	ND	0.11 ± 0.04	0.38 ± 0.05
P3 F antagomir	ND	0.11 ± 0.22	0.29 ± 0.005

The data are expressed as fold change ($2^{-\Delta\Delta CT}$) normalized to the level of expression in the P2 liver. The data are the average of six independent measurements ± SEM. ND, none detected.

bile ductular differentiation. We hypothesized that knockdown of miR-23b polycistron miRNAs in the fetal liver would promote TGF- β signaling, leading to an increase in hepatoblast commitment to the bile ductular phenotype. To test this, we developed a protocol to individually inject E16.5 fetuses with either PBS or an antagomir mix against the miR-23b polycistron miRNAs in separate pregnant females (see Materials and Methods).

We assayed the effects of injection on the livers of fetuses at birth by staining the livers with the bile duct pan-cytokeratin antibody that preferentially stains developing bile ducts (Fig. 2). As shown in Figure 2A and B, cytokeratin staining (reddish-brown stain) of PBS-injected livers was limited to portal triads in postnatal day 1 livers. However, antagomir-injected livers revealed massive expression of cytokeratin throughout large sections of liver (Fig. 2C and E). High magnification of the positive cells revealed strong staining in primitive ductular elements in the livers (Fig. 2D and F). RNA extraction of early postnatal livers confirmed that the levels of all three miRNAs were significantly reduced (Table 1). These data supported our hypothesis that reduction of the miR-23b miRNAs would increase TGF- β signaling and push fetal liver stem cells toward the bile ductular phenotype.

We also assayed the effect of antagomir injection on the proliferation of hepatocytes by measuring Ki-67⁺ nuclei in postnatal mice. An example of this stain is shown in Figure 3. This confirmed that hepatocyte proliferation was 49% ($p = 1.6 \times 10^{-63}$) lower in antagomir-treated mice versus PBS-injected mice (Table 2). In contrast, labeling of bile ducts was not affected. A 44% ($p = 8.6 \times 10^{-46}$) reduction in hepatocyte proliferation in antagomir-injected fetuses was also detected by BrdU injection of newborns and assay of BrdU⁺ nuclei 1 day later (Table 3). The above experiments supported the overall hypothesis that antagomir injection blocks miR targeting of Smads, allows TGF- β signaling in hepatocytes, and inhibits their proliferation while allowing TGF- β to promote ductular differentiation.

Antagomir Treatment Blocks Fibrotic Change in TGF- β 1 Transgenic Mouse Liver

The Alb/TGF- β 1 transgenic mouse model, developed by the S. Thorgeirsson laboratory, provides another model to test the effectiveness of miR-23b polycistron antagomirs on TGF- β effects on the liver³⁶. The Alb/TGF- β 1 transgene is located on the Y chromosome. Only male mice overexpress TGF- β in the liver and develop liver fibrosis during the first month of life³⁶. Female littermates served as controls.

To test the effects of miR-23b cluster knockdown on postnatal liver growth and differentiation, we injected (IP) our mixture of antagomirs against miR-23b, miR-27b, and miR-24 by IP on postnatal day 1. On postnatal day 20, control and experimental male and female mice were injected with BrdU and sacrificed a day later. Quantitation of the average number of BrdU⁺ hepatocyte nuclei per 10 \times field revealed a 33% ($p = 1.27 \times 10^{-21}$) reduction in proliferation in antagomir-injected male Alb/TGF- β mice compared to the PBS-injected littermate controls, demonstrating the significant increase in the inhibitory activity

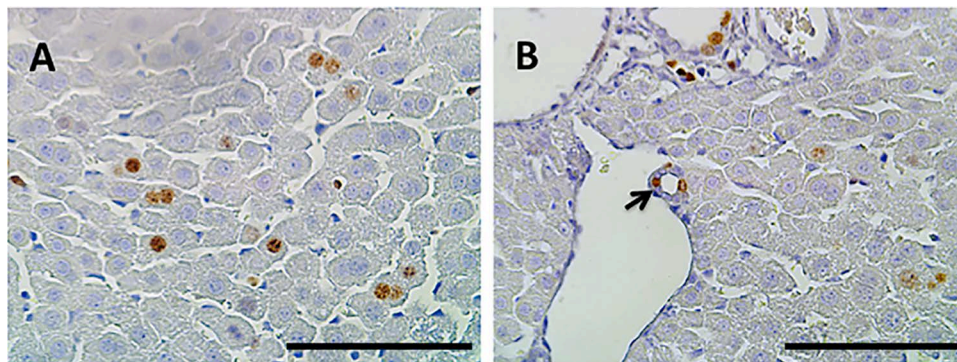


Figure 3. Ki-67 staining of liver sections. (A) Example of nuclear Ki-67 staining of hepatocytes in the 3-week-old mouse liver. (B) Example of nuclear Ki-67 staining of cholangiocytes in bile duct in the 3-week-old mouse liver. This staining of proliferative cells is quantified in Table 2. Ki-67 staining is detected by brown staining. Scale bars: 100 μ m.

Table 2. Effects of IP Injection of Postnatal Day 1 Swiss Webster Pups With Antagomir Mix

Injection	Hepatocytes	Bile Ducts
PBS	10.13 ± 0.2	1.13 ± 0.1
Antagomir mix	5 ± 0.2*	1.06 ± 0.1**

Ki-67 staining carried out on 3-week fixed tissues to determine effects of antagomirs on proliferation of hepatocytes and bile duct cells. IP injection of antagomirs was performed at postnatal day 1. Pups were sacrificed at 3 weeks. Tissue processing and staining are as described in Materials and Methods. Data are the number of positive nuclei per 40× field.

Student's *t*-test: * $p < 0.0001$, ** $p = 0.34$.

of TGF- β on hepatocyte growth in antagomir-treated liver (Table 4). BrdU staining of antagomir-injected female mice revealed a 7% ($p = 0.005$) reduction in hepatocyte nuclear staining, due to the documented presence of endogenous miR-23b polycistron miRNAs in normal liver. Thus, we expected an additional (~6%) reduction in the antagomir-treated male transgenic mice. However, we observed an additional 30% reduction, suggesting a synergistic effect of removing the miR-23b cluster miRNAs increasing the biological activity of TGF- β in the transgenic mouse livers.

We stained the livers from the above experiment with pan-cytokeratin antibody to look for phenotypic effects on bile ductular differentiation. Overall the portal tracts were generally normal. However, in the antagomir-treated male mice, we observed localized regions of primitive bile ductular differentiation in peripheral parenchymal (non-portal tract) regions of the liver (Fig. 4). The unusual duct-like structures were highly prevalent and unorganized compared to normal bile ducts that are only located in portal tracts. Similar alterations were not observed in any of the control transgenic or nontransgenic livers. Biliary morphogenesis is ongoing in the periphery of the early postnatal liver; thus, only peripheral regions in the postnatal livers were susceptible to overt antagomir effects, producing ductular differentiation.

Table 3. Effects of Injection of E16.5 Fetuses With Antagomir Mix on BrdU Labeling of Hepatocyte Nuclei at Birth

Treatment	BrdU Labeling of Hepatocyte Nuclei
PBS	10.5 ± 0.6
Antagomir mix	4.7 ± 0.4*

IP injection of antagomirs was performed at postnatal day 1. Pups were sacrificed at 3 weeks following a 1-h pulse of BrdU labeling. Tissue processing and staining are as described in Materials and Methods. Data are positive nuclei per 40× field.

* $p = 8.6 \times 10^{-46}$.

Table 4. Effects of Antagomir Mix Injection on Postnatal Day 1, on the Proliferation of Hepatocytes in Male Alb/TGF- β Transgenic Mice and Female Littermate Control Mice

Treatment	Female	Male
PBS	24.55 ± 0.5	16.69 ± 0.4
Antagomir mix	22.8 ± 0.4*	11.41 ± 0.2**

Experimental approach similar to that in Table 2 except for mouse strain and BrdU assay. Antagomir injection was on postnatal day 1 and BrdU injection on postnatal day 20 followed by sacrifice on postnatal day 21. Data are positive hepatocyte nuclei per 40× field.

Student's *t*-test: * $p = 0.005$ versus female PBS control; ** $p = 1.27 \times 10^{-21}$ versus male PBS control.

TGF- β is a potent inducer of liver fibrosis³⁷. Alb/TGF- β male mice develop liver fibrosis beginning at 2 weeks of age, and this increases in the early months of life³⁶. Male Alb/TGF- β and control female mice were injected with antagomirs or PBS on postnatal day 1 to examine the effect of the antagomir mix on the onset of fibrosis. Since antagomirs have been shown to be effective in the liver for a month, we assayed for the effects of injection on postnatal day 20. Fibrosis in these livers was visualized using reticulin staining of collagen fibers. Analysis of reticulin fibers revealed a dramatic increase in reticulin fibers (black lines following a sinusoidal pattern), indicating the onset of fibrosis in male TGF- β liver (Fig. 5B) compared to female control liver (Fig. 5A). Antagomir mix-injected female livers also had very little reticulin staining (Fig. 5C). However, antagomir injection caused a dramatic decrease in reticulin fiber abundance in the male TGF- β liver (Fig. 5D). A parallel set of mutant antagomirs (mm-antagomirs) with mutated seed sites were much less effective in reducing the abundance of reticulin fibers in male liver versus female control liver [Fig. 5E (female) and F (male)].

To quantitate the effect of antagomir treatment reticulin fiber length, we used ImageJ (NIH). This revealed a 79% reduction in reticulin fibril length down to the normal level after antagomir injection of male TGF- β mice (Fig. 6). In contrast, TGF- β mice injected with the mm-antagomirs with mutated seed sites were much less effective, causing only a 26% reduction in the length of reticulin fibers (Fig. 6). Female animals that do not express the TGF- β transgene antagomirs and mutant antagomirs reduced the reticulin fibers by 39% (Fig. 6).

In addition to classic antagomirs, a second type of anti-miRNA is locked nucleic acid (LNA) inhibitors. These anti-miRNAs contain modified LNA nucleotides that are RNase resistant and allow long-term inactivation of miRNAs in the liver^{38,39}. To determine if treatment with LNA inhibitors would allow the resolution of fibrosis that had already developed in male alb/TGF- β animals, we

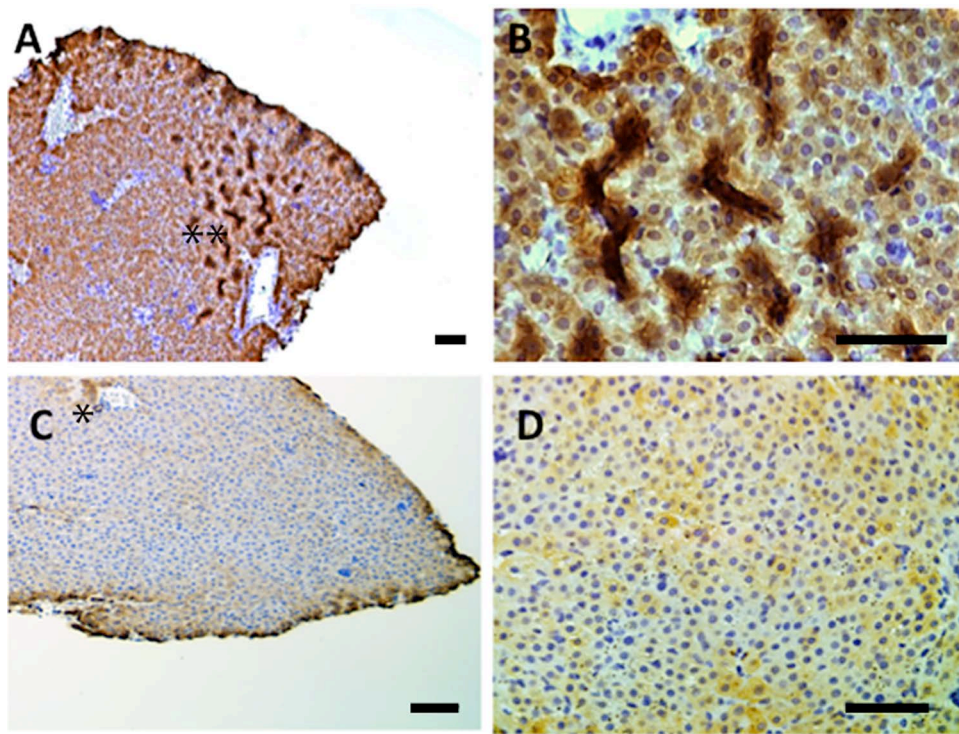


Figure 4. Effects of antagomir mix injection of TGF- β^+ male on cytochrome staining of peripheral liver segments. (A) Low magnification of a large section of antagomir-injected liver revealing pattern of increased cytochrome staining at the periphery of liver section. **The region containing the increased cytochrome staining in duct-like structures. (B) High magnification of boxed section in (A) revealing increased cytochrome staining (brown) in highly prevalent bile duct-like structures. (C) Low magnification of PBS-injected liver. *A cytochrome-positive bile duct. (D) High magnification of PBS-injected liver. Scale bars: 100 μ m.

injected 2-week-old Alb/TGF- β male and control female mice with the LNA inhibitors. Sirius Red staining was used to visualize collagen deposition in the fibrotic scar at 1 month old. Female mice showed staining localized to the portal region as expected [Fig. 7A (low magnification) and D (high magnification)]; however, male transgenic mice showed massive collagen staining both in the portal tract and throughout the parenchyma. The increased staining was specifically located in a pattern similar to the reticulin staining that marks sinusoids where collagen accumulates. This served as a second marker for fibrosis in the Alb/TGF- β male mice [Fig. 7B (low magnification) and E (high magnification)]. Remarkably, LNA antagomir-treated male transgenic mice showed an almost complete elimination of Sirius Red staining in the sinusoids, while staining remained in the portal tracts [Fig. 7C (low magnification) and F (high magnification)].

Inhibition of miR-23b Cluster miRNAs Restores Vitamin A Fluorescence to In Vitro-Activated Murine Hepatic Stellate Cells

In order to further investigate the cellular basis for the effect of antagomir treatment, we isolated murine HSCs. When placed in culture, these cells spontaneously

activate and lose their characteristic vitamin A fluorescence (Fig. 8A–D). The level of miR-27b is elevated in these cells, while miR-23b and miR-24 are reduced (Fig. 8E). Antagomir treatment of the activated cells reduced the levels of miR-23b, miR-27b, and miR-24 in the cells by 90%, and this was accompanied by restoration of vitamin A fluorescence in the cells (Fig. 9A–E).

As HSCs become activated through an epithelial-to-mesenchymal transition, they lose the ability to store vitamin A in the form of retinol esters, mainly retinyl palmitate^{23,40,41}. In a further experiment, we treated activated human LX2 stellate cells with a palmitic acid and retinol mix that causes reversion and the reestablishment of the quiescent state⁴². The combination treatment of LX2 cells with retinol and palmitic acid restored the ability of the cells to uptake lipid droplets (Fig. 10A and B). This treatment was also accompanied by the reduction in the expression of ColA1 and ACTA2, both markers of activated stellate cells (Fig. 10C and D). Furthermore, when the LX2 cells are reverted by treatment with palmitic acid and retinol (PARA), the levels of miR-23b and miR-27b are significantly reduced (Fig. 11).

We next tested whether knocking down miR-23b polycistron miRNA in LX2 cells would mimic the effects of

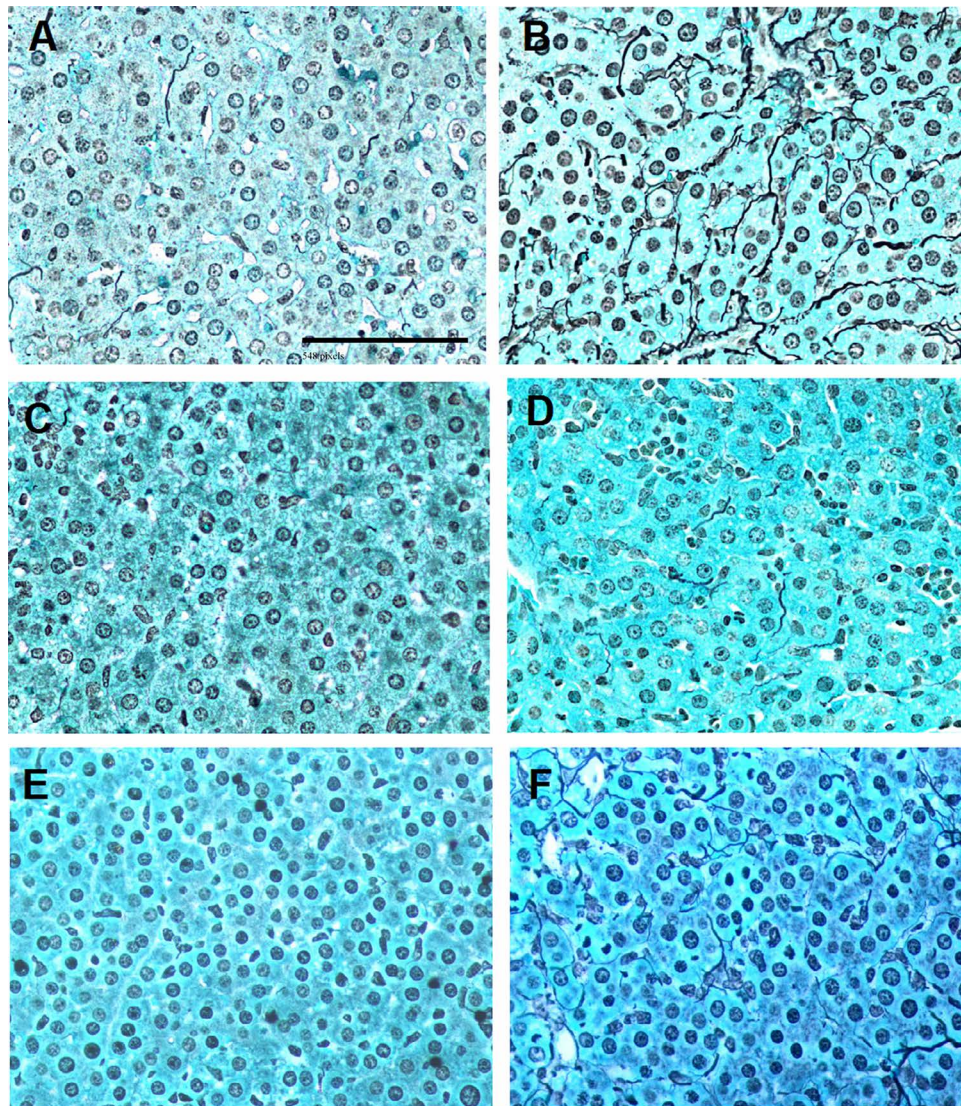


Figure 5. The effects of antagomir injection on the onset of fibrosis measured by reticulin staining in livers. (A) PBS injection of female mice ($TGF-\beta^+$). (B) PBS injection of male $TGF-\beta$ mice reveals abundant reticulin staining. (C) Antagomir injection of female mice. (D) Antagomir injection of male $TGF-\beta$ mice reveals dramatic reduction of reticulin staining. (E) mm-Antagomir injection of female mice. (F) mm-Antagomir injection of male $TGF-\beta$ mice reveals abundant reticulin staining. Scale bar: 100 μm .

palmitic acid and retinol on gene expression. For this we used miR-Zip plasmids that express anti-miRs against each of the miR23b cluster miRNAs. We transfected these anti-miR expression plasmids separately and in combination and measured their effect on ColA1 and ACTA2 expression. The individual miR-Zip plasmids had variable effects, but the combination of all three plasmids caused a significant reduction in the expression of both ColA1 and ACTA2 (Fig. 12). In addition, the level of MMP1 expression was dramatically increased by treatment with miR-23b, miR-27b, and the combination of all three miR-Zips (Fig. 13). These data support the hypothesis that miR-23b polycistron miRNAs also can promote

reversion to quiescence of human stellate cells by altering the level of key genes needed for the activated state.

DISCUSSION

miRNA profiling studies have shown that a number of miRNAs are regulated as a result of liver injury and fibrosis⁴³. These miRNAs can be divided into two groups: antifibrogenic miRNAs, which are commonly downregulated following the onset of fibrosis, or profibrogenic miRNAs, which are upregulated in fibrotic liver⁴³. Several of the antifibrogenic miRNAs reduce $TGF-\beta$ signaling by targeting intermediate signaling molecules, Smad4 and Smad2/3, the inhibitory Smad7, or $TGF-\beta$ receptors⁴³⁻⁴⁶.

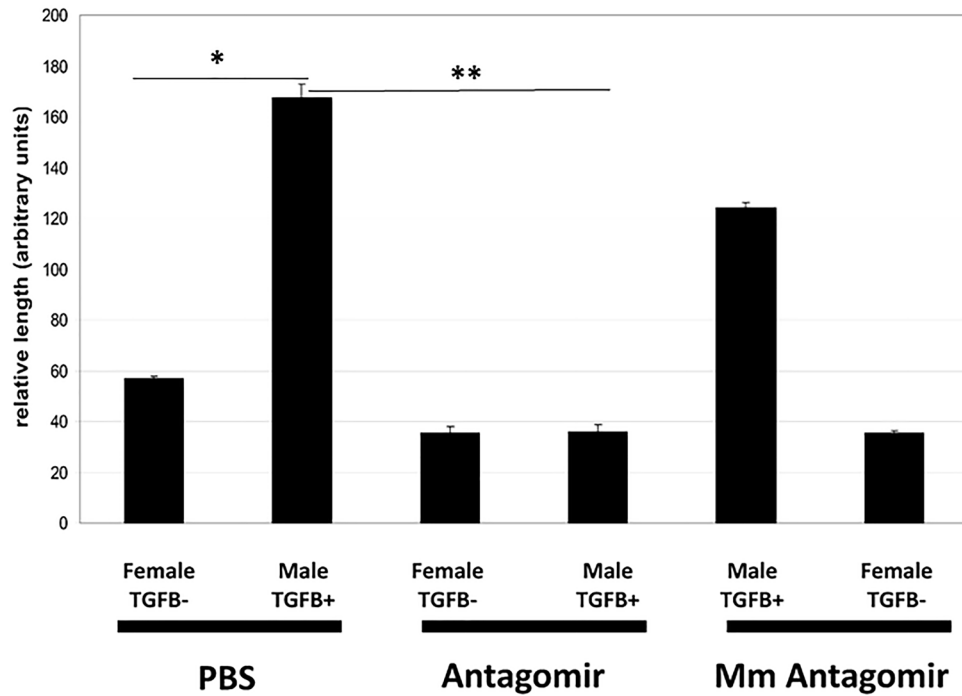


Figure 6. Quantitation of reticulin fiber length in PBS-, antagomir-, and mm-antagomir-injected female and male Alb/TGF- β mice. Relative length of reticulin fibers was determined using ImageJ (NIH). Values are the mean \pm SEM of the length of reticulin fibers. Five animals were analyzed/group and 10 fields 20 \times were analyzed/animal. * $p=0.0003$, ** $p=0.002$.

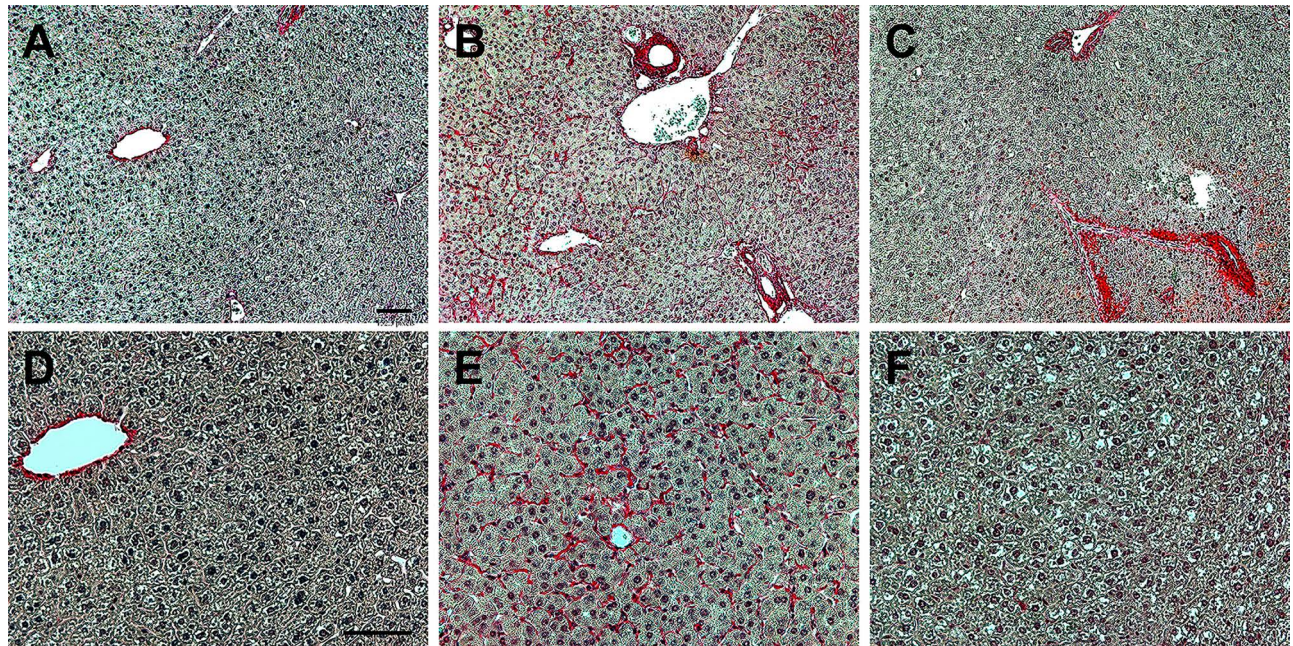


Figure 7. Effects of injection of LNA antagomirs on collagen deposition in control and TGF- β mice detected by Sirius Red staining of livers. (A, D) Normal collagen deposition detected in female TGF- β ⁻ mouse liver. (B, E) Fibrotic deposition of collagen detected throughout male TGF- β ⁺ mouse liver. (C, F) Reversal of fibrotic deposition of collagen in liver in LNA antagomir-injected male TGF- β mice as judged by the lack of Sirius Red staining in parenchyma. Scale bars: 100 μ m.

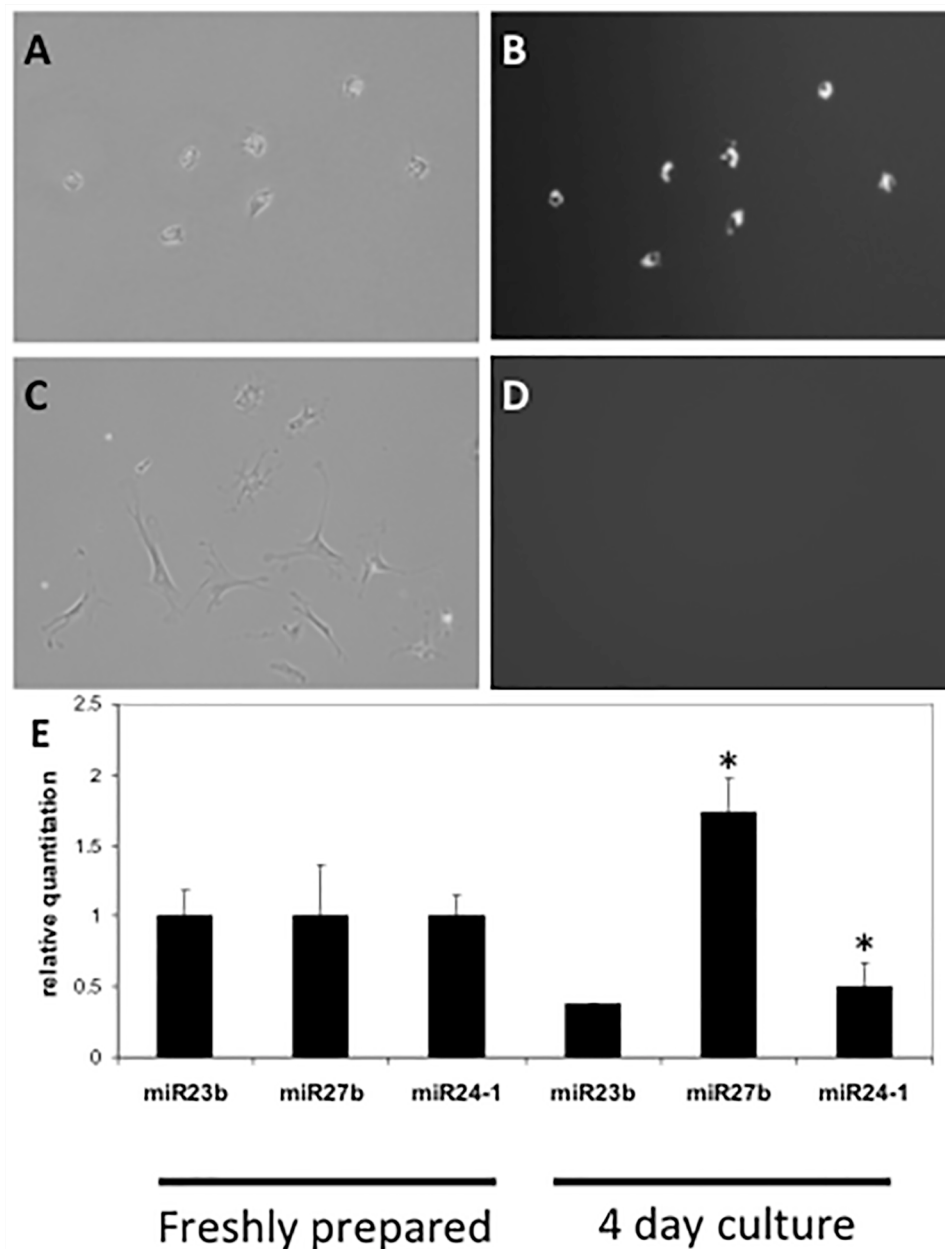


Figure 8. (A, B) Freshly isolated murine hepatic stellate cells under phase contrast (A) and UV fluorescence microscopy (B) showing vitamin A fluorescence in freshly plated cells. (C, D) The cells in (A) and (B) after 4 days of culture showing loss of vitamin A fluorescence. (E) Graph depicting the increase in miR-27b and decrease in miR-23b and miR-24-1 in hepatic stellate cells after 4 days of culture. Levels of each miR in freshly isolated cells were used as a 100% reference. * $p=0.01$.

One example is miR-29, which is downregulated in response to TGF- β ⁴⁷⁻⁵⁰. Several profibrogenic miRNAs or “fibromirs” that are upregulated in fibrosis are also regulated by TGF- β ^{43,51-53}. Examples of these miRNAs include miR-21, miR-17-5p, and miR-181b^{43,51,52}. These examples reveal additional complex miRNA-driven gene regulation changes that occur during fibrosis, in addition to the ones described in this report.

The murine fetal injection of miRNA antagonists in this report revealed dramatic effects on fetal liver structure and gene expression. The experiments showed that knocking down the set of miR-23b polycistronic miRNAs alters gene expression and cell differentiation toward the bile ductular lineage in late fetal liver. The data support our working hypothesis, which proposes that as miR-23b cluster miRNAs are expressed at high

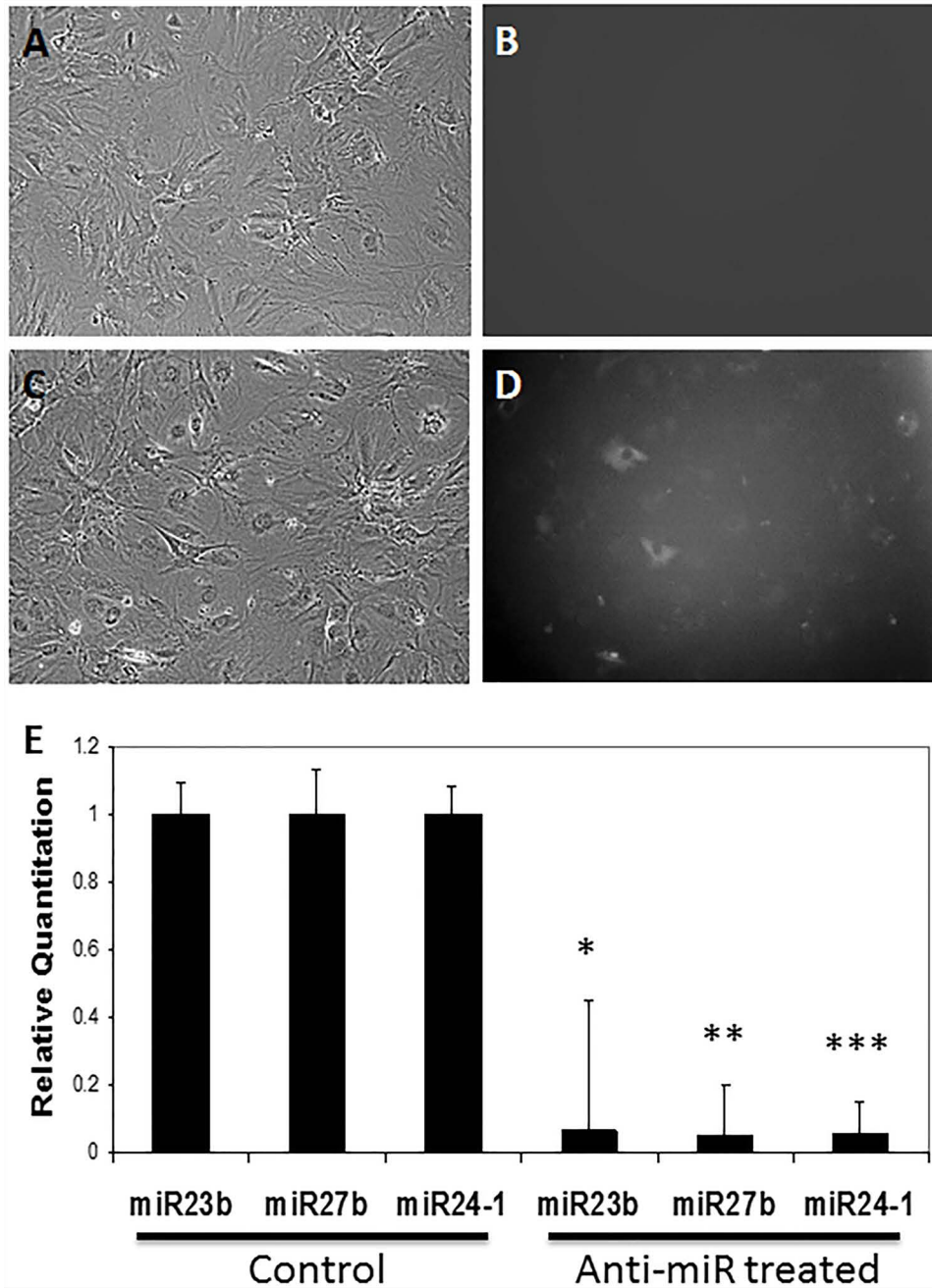


Figure 9. Inhibition of miR-23b cluster miRNAs restores vitamin A fluorescence to in vitro-activated murine hepatic stellate cells. (A) Phase contrast of mock-transfected control cells. (B) UV fluorescence of mock-transfected control cells. (C) Phase contrast of antagomir-transfected cells. (D) UV fluorescence of antagomir-transfected cells revealing restoration of vitamin A fluorescence is seen in substantial proportion of cells. (E) Graph depicting the reduction of miR-23b, miR-24-1, and miR-27b determined by TaqMan qPCR. * $p=0.05$, ** $p=0.01$, $p=0.008$.

levels, TGF- β signaling molecules are targeted, TGF- β signaling is blocked, and the developing hepatocytes are able to proliferate. In contrast, low levels of these same miRNAs caused by our antagomir injections promote TGF- β -induced bile duct morphogenesis. This supports a model that cell fate decisions are actively occurring

in the fetal liver through its later stages of development and demonstrate the plasticity of cell fate decisions in the neonatal livers.

In this report, we have used the Alb/TGF- β transgenic mouse model of liver fibrosis to develop a protocol for in vivo investigation of molecular controls of liver

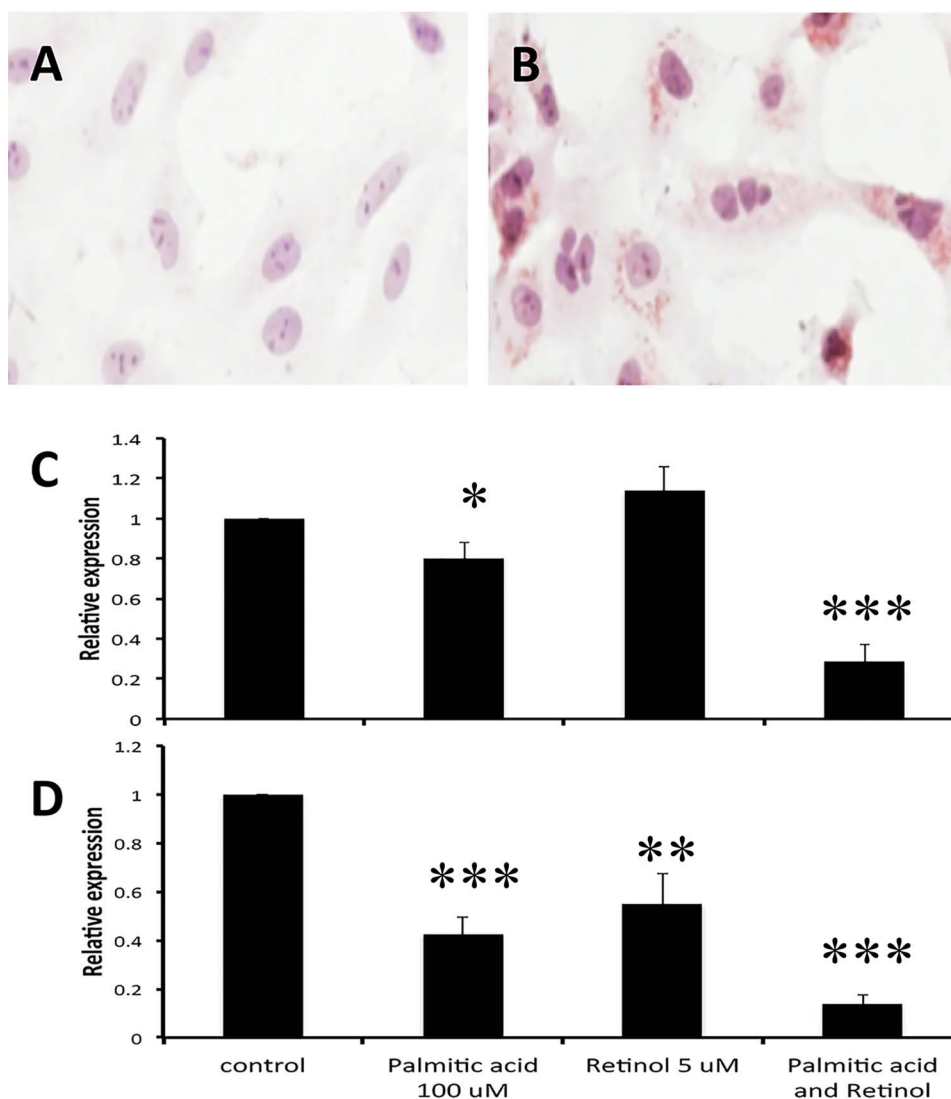


Figure 10. Reversion of LX2 cells by palmitic acid and retinoic acid. (A) Lack of Oil red O staining of activated LX2 cells. (B) Induction of Oil red O staining in LX2 cells by treatment with palmitic acid and retinol, indicating switch to quiescent state of LX2 cells. (C) Reductions in COL1A1 expression by treatments with palmitic acid and retinol alone and in combination as indicated. (D) Reductions in ACTA2 expression by treatments with palmitic acid and retinol alone and in combination as indicated. qRT-PCR data are expressed as relative expression calculated using a $2^{-\Delta\Delta CT}$. The data represent the mean of nine determinations \pm SEM. * $p < 0.05$, ** $p < 0.01$, *** $p < 0.001$.

fibrosis³⁶. Direct injection of antagonirs caused a major blockage of fibrosis at 1 month old. Furthermore, injections with a second type of anti-miR, LNA inhibitors that contain modified locked nucleic acid nucleotides, were also effective and were able to cause reversion of fibrosis that had been established in the liver.

Causes of fibrosis that precede cirrhosis include chronic viral hepatitis B (CHB), chronic hepatitis C (CHC), nonalcoholic fatty liver disease (NAFLD), and/or alcoholic liver disease (ALD)^{13,23,54}. No effective treatments currently exist, and there is a need for targeted treatments for reversal of fibrosis in a tissue, including

fibrosis of the liver. In response to liver injury associated with the above etiologies, HSCs undergo an “activation” process in which they lose vitamin A, become highly proliferative, and synthesize “fibrotic” matrix rich in type I collagen, and fibrosis ensues¹⁶. Our in vitro investigations with LX2 cells, testing the effects of lentiviral-based miRNA inhibitors (miR-Zips), showed that the inhibition of 23 polycistron miRNAs could restore quiescence to activated stellate cells. This provides a cellular model for the antifibrotic effects we observed in Alb/TGF- β mice and demonstrated the expected cell type-dependent effects of antagonirs in the complex cellular milieu of

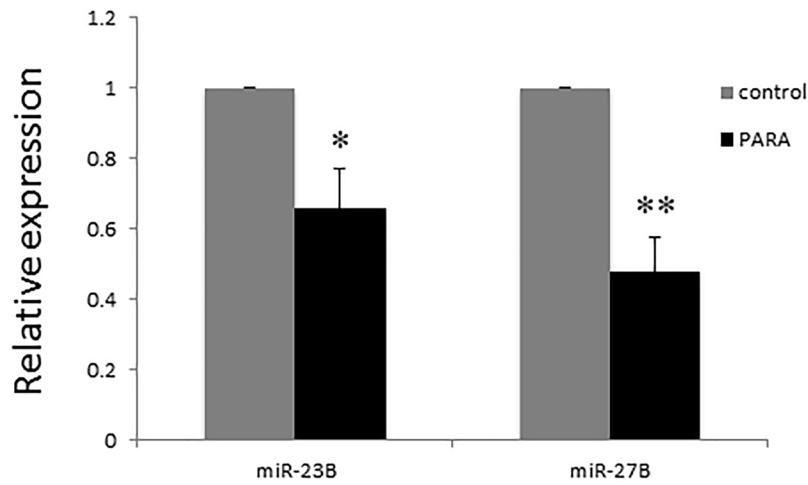


Figure 11. Effects of palmitic acid and retinol treatment on miR-23b and miR-27b expression in LX2 cells. Untreated LX2 cells (gray bars, control). LX2 cells treated with the combination of palmitic acid and retinol (black bars, PARA) as described in Materials and Methods. qRT-PCR data are expressed as relative expression calculated using $2^{-\Delta\Delta CT}$. The data represent the mean of nine determinations \pm SEM. * $p < 0.05$, ** $p < 0.01$.

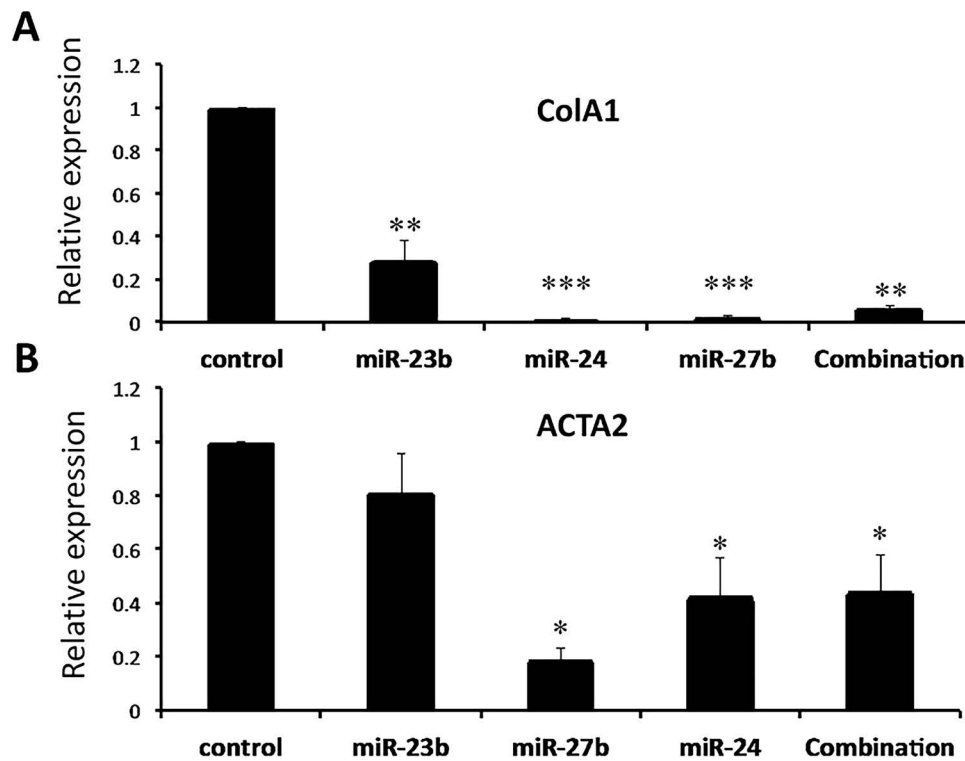


Figure 12. The effects of miR-Zip, anti-miR, and vectors on the expression of (A) ColA1 or (B) ACTA2 in LX2 cells. Plasmids expressing anti-miRs against miR-23b, miR-24, and miR-27b were transfected individually and in triple combination into LX2 cells, and gene expression was determined by qRT-PCR as described in Materials and Methods. * $p < 0.05$, ** $p < 0.001$, *** $p < 0.005$.

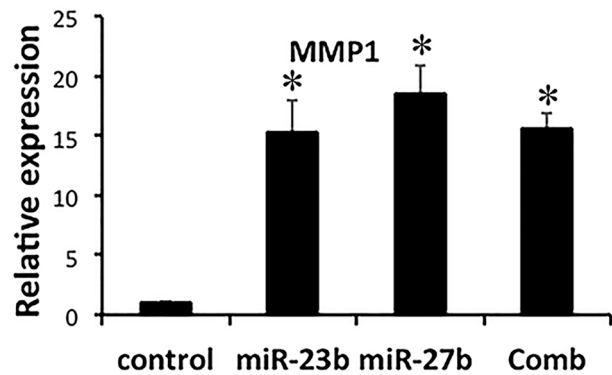


Figure 13. The effects of miR-Zip, anti-miR, and vectors on the expression of MMP1. Plasmids expressing anti-miRs against miR-23b and miR-27b were transfected individually and in triple combination with miR-24 and miR-Zip into LX2 cells, and gene expression was determined by qRT-PCR as described in Materials and Methods. * $p < 0.05$.

the liver. The main cell type affected in the fetal injection is most likely hepatoblasts, and the most likely cells targeted in the postnatal injection are hepatocytes and hepatoblasts at the periphery of the liver where bile duct differentiation is still occurring. In the Alb/TGF- β mice, the most likely targets are stellate cells in the liver. While the initial cause of the fibrosis is varied, the ultimate mechanism of fibrosis is common and is treatable with the methods described in this report. The antagonirs and LNAs used in our protocol can be administered in a pharmaceutically acceptable carrier.

ACKNOWLEDGMENTS: The authors would like to thank the Histopathology Core and Analytic Imaging Facility. We also thank Dr. M. Bitzer for the gift of LNA anti-miRs, Dr. S. Thorgeirsson for the permission to use the Alb/TGF- β line 25 transgenic mice in this work, and Dr. S. Friedman for the LX2 cells. Research support was from NYSTEM FAU#0804180400 (C.E.R.) and NYSTEM CO28172 (L.E.R.) and by NIH grants RO1 CA 37232-28 (C.E.R.) and P30 DK 41296-24 (A.W.). The authors declare no conflicts of interest.

REFERENCES

- Bartel DP. MicroRNAs: Genomics, biogenesis, mechanism, and function. *Cell* 2004;116(2):281–97.
- Mukherji S, Ebert MS, Zheng GX, Tsang JS, Sharp PA, van Oudenaarden A. MicroRNAs can generate thresholds in target gene expression. *Nat Genet* 2011;43(9):854–9.
- Selbach M, Schwanhaussner B, Thierfelder N, Fang Z, Khanin R, Rajewsky N. Widespread changes in protein synthesis induced by microRNAs. *Nature* 2008;455(7209):58–63.
- Rogler CE, Levoci L, Ader T, Massimi A, Tchaikovskaya T, Norel R, Rogler LE. MicroRNA-23b cluster microRNAs regulate transforming growth factor-beta/bone morphogenetic protein signaling and liver stem cell differentiation by targeting Smads. *Hepatology* 2009;50(2):575–84.
- Yi R, Poy MN, Stoffel M, Fuchs E. A skin microRNA promotes differentiation by repressing ‘stemness’. *Nature* 2008;452(7184):225–9.
- Poy MN, Eliasson L, Krutzfeldt J, Kuwajima S, Ma X, Macdonald PE, Pfeffer S, Tuschl T, Rajewsky N, Rorsman P, Stoffel M. A pancreatic islet-specific microRNA regulates insulin secretion. *Nature* 2004;432(7014):226–30.
- Lemaigre FP. Development of the biliary tract. *Mech Dev* 2003;120(1):81–7.
- Clotman F, Jacquemin P, Plumb-Rudewicz N, Pierreux CE, Van der Smissen P, Dietz HC, Courtoy PJ, Rousseau GG, Lemaigre FP. Control of liver cell fate decision by a gradient of TGF beta signaling modulated by Onecut transcription factors. *Genes Dev* 2005;19(16):1849–54.
- Clotman F, Lemaigre FP. Control of hepatic differentiation by activin/TGFbeta signaling. *Cell Cycle* 2006;5(2):168–71.
- Ader T, Norel R, Levoci L, Rogler LE. Transcriptional profiling implicates TGFbeta/BMP and Notch signaling pathways in ductular differentiation of fetal murine hepatoblasts. *Mech Dev* 2006;123(2):177–94.
- Friedman SL. Molecular regulation of hepatic fibrosis, an integrated cellular response to tissue injury. *J Biol Chem* 2000;275(4):2247–50.
- Bataller R, Brenner DA. Liver fibrosis. *J Clin Invest* 2005;115(2):209–18.
- Iwaisako K, Brenner DA, Kisseleva T. What’s new in liver fibrosis? The origin of myofibroblasts in liver fibrosis. *J Gastroenterol Hepatol* 2012;27(Suppl 2):65–8.
- Wells RG, Kruglov E, Dranoff JA. Autocrine release of TGF-beta by portal fibroblasts regulates cell growth. *FEBS Lett* 2004;559(1–3):107–10.
- Dranoff JA, Wells RG. Portal fibroblasts: Underappreciated mediators of biliary fibrosis. *Hepatology* 2010;51(4):1438–44.
- Geerts A. History, heterogeneity, developmental biology, and functions of quiescent hepatic stellate cells. *Semin Liver Dis* 2001;21(3):311–35.
- Blomhoff R, Holte K, Naess L, Berg T. Newly administered [3H]retinol is transferred from hepatocytes to stellate cells in liver for storage. *Exp Cell Res* 1984;150(1):186–93.
- Senoo H, Kojima N, Sato M. Vitamin A-storing cells (stellate cells). *Vitam Horm* 2007;75:131–59.
- Friedman SL. Hepatic stellate cells. *Prog Liver Dis* 1996;14:101–30.
- Schirmacher P, Geerts A, Jung W, Pietrangolo A, Rogler CE, Dienes HP. The role of Ito cells in the biosynthesis of HGF-SF in the liver. *EXS* 1993;65:285–99.
- Friedman SL. Hepatic stellate cells: Protean, multifunctional, and enigmatic cells of the liver. *Physiol Rev* 2008;88(1):125–72.
- Mederacke I, Dapito DH, Affo S, Uchinami H, Schwabe RF. High-yield and high-purity isolation of hepatic stellate cells from normal and fibrotic mouse livers. *Nat Protoc* 2015;10(2):305–15.
- Friedman SL. Mechanisms of hepatic fibrogenesis. *Gastroenterology* 2008;134(6):1655–69.
- Yin C, Evason KJ, Asahina K, Stainier DY. Hepatic stellate cells in liver development, regeneration, and cancer. *J Clin Invest* 2013;123(5):1902–10.
- Kisseleva T, Brenner DA. Fibrogenesis of parenchymal organs. *Proc Am Thorac Soc* 2008;5(3):338–42.

26. Bissell DM. Chronic liver injury, TGF-beta, and cancer. *Exp Mol Med*. 2001;33(4):179–90.
27. Derynck R, Zhang Y, Feng XH. Smads: Transcriptional activators of TGF-beta responses. *Cell* 1998;95(6):737–40.
28. Heldin CH, Miyazono K, ten Dijke P. TGF-beta signalling from cell membrane to nucleus through SMAD proteins. *Nature* 1997;390(6659):465–71.
29. Shi Y, Massague J. Mechanisms of TGF-beta signaling from cell membrane to the nucleus. *Cell* 2003;113(6):685–700.
30. Wrana JL. Crossing Smads. *Sci STKE* 2000;2000(23):re1.
31. Wrighton KH, Lin X, Feng XH. Phospho-control of TGF-beta superfamily signaling. *Cell Res*. 2009;19(1):8–20.
32. Friedman SL. Seminars in medicine of the Beth Israel Hospital, Boston. The cellular basis of hepatic fibrosis. Mechanisms and treatment strategies. *N Engl J Med*. 1993;328(25):1828–35.
33. Pinzani M, Marra F. Cytokine receptors and signaling in hepatic stellate cells. *Semin Liver Dis*. 2001;21(3):397–416.
34. Xu L, Hui AY, Albanis E, Arthur MJ, O'Byrne SM, Blaner WS, Mukherjee P, Friedman SL, Eng FJ. Human hepatic stellate cell lines, LX-1 and LX-2: New tools for analysis of hepatic fibrosis. *Gut* 2005;54(1):142–51.
35. Rehmsmeier M. Prediction of microRNA targets. *Methods Mol Biol*. 2006;342:87–99.
36. Sanderson N, Factor V, Nagy P, Kopp J, Kondaiah P, Wakefield L, Roberts AB, Sporn MB, Thorgeirsson SS. Hepatic expression of mature transforming growth factor beta 1 in transgenic mice results in multiple tissue lesions. *Proc Natl Acad Sci USA* 1995;92(7):2572–6.
37. Meindl-Beinker NM, Matsuzaki K, Dooley S. TGF-beta signaling in onset and progression of hepatocellular carcinoma. *Dig Dis*. 2012;30(5):514–23.
38. Lennox KA, Behlke MA. Chemical modification and design of anti-miRNA oligonucleotides. *Gene Ther*. 2011;18(12):1111–20.
39. Gao S, Dagnaes-Hansen F, Nielsen EJ, Wengel J, Besenbacher F, Howard KA, Kjems J. The effect of chemical modification and nanoparticle formulation on stability and biodistribution of siRNA in mice. *Mol Ther*. 2009;17(7):1225–33.
40. Yamada M, Blaner WS, Soprano DR, Dixon JL, Kjeldbye HM, Goodman DS. Biochemical characteristics of isolated rat liver stellate cells. *Hepatology* 1987;7(6):1224–9.
41. Moriwaki H, Blaner WS, Piantedosi R, Goodman DS. Effects of dietary retinoid and triglyceride on the lipid composition of rat liver stellate cells and stellate cell lipid droplets. *J Lipid Res*. 1988;29(11):1523–34.
42. Lee TF, Mak KM, Rackovsky O, Lin YL, Kwong AJ, Loke JC, Friedman SL. Downregulation of hepatic stellate cell activation by retinol and palmitate mediated by adipose differentiation-related protein (ADRP). *J Cell Physiol*. 2010;223(3):648–57.
43. Kitano M, Bloomston PM. Hepatic stellate cells and microRNAs in pathogenesis of liver fibrosis. *J Clin Med*. 2016;5(3).
44. Tu X, Zhang H, Zhang J, Zhao S, Zheng X, Zhang Z, Zhu J, Chen J, Dong L, Zang Y, Zhang J. MicroRNA-101 suppresses liver fibrosis by targeting the TGFbeta signalling pathway. *J Pathol*. 2014;234(1):46–59.
45. Tu X, Zheng X, Li H, Cao Z, Chang H, Luan S, Zhu J, Chen J, Zang Y, Zhang J. MicroRNA-30 protects against carbon tetrachloride-induced liver fibrosis by attenuating transforming growth factor beta signaling in hepatic stellate cells. *Toxicol Sci*. 2015;146(1):157–69.
46. He Y, Huang C, Zhang SP, Sun X, Long XR, Li J. The potential of microRNAs in liver fibrosis. *Cell Signal*. 2012;24(12):2268–72.
47. Ogawa T, Iizuka M, Sekiya Y, Yoshizato K, Ikeda K, Kawada N. Suppression of type I collagen production by microRNA-29b in cultured human stellate cells. *Biochem Biophys Res Commun*. 2010;391(1):316–21.
48. Huang YH, Tiao MM, Huang LT, Chuang JH, Kuo KC, Yang YL, Wang FS. Activation of mir-29a in activated hepatic stellate cells modulates its profibrogenic phenotype through inhibition of histone deacetylases 4. *PLoS One* 2015;10(8):e0136453.
49. Bandyopadhyay S, Friedman RC, Marquez RT, Keck K, Kong B, Icardi MS, Brown KE, Burge CB, Schmidt WN, Wang Y, McCaffrey AP. Hepatitis C virus infection and hepatic stellate cell activation downregulate miR-29: miR-29 overexpression reduces hepatitis C viral abundance in culture. *J Infect Dis*. 2011;203(12):1753–62.
50. Kwiecinski M, Noetel A, Elfimova N, Trebicka J, Schievenbusch S, Strack I, Molnar L, von Brandenstein M, Tox U, Nischt R, Coutelle O, Dienes HP, Odenthal M. Hepatocyte growth factor (HGF) inhibits collagen I and IV synthesis in hepatic stellate cells by miRNA-29 induction. *PLoS One* 2011;6(9):e24568.
51. Yu F, Guo Y, Chen B, Dong P, Zheng J. MicroRNA-17-5p activates hepatic stellate cells through targeting of Smad7. *Lab Invest*. 2015;95(7):781–9.
52. Zhang Z, Zha Y, Hu W, Huang Z, Gao Z, Zang Y, Chen J, Dong L, Zhang J. The autoregulatory feedback loop of microRNA-21/programmed cell death protein 4/activation protein-1 (MiR-21/PDCD4/AP-1) as a driving force for hepatic fibrosis development. *J Biol Chem*. 2013;288(52):37082–93.
53. Zheng J, Wu C, Xu Z, Xia P, Dong P, Chen B, Yu F. Hepatic stellate cell is activated by microRNA-181b via PTEN/Akt pathway. *Mol Cell Biochem*. 2015;398(1–2):1–9.
54. Hernandez-Gea V, Friedman SL. Pathogenesis of liver fibrosis. *Annu Rev Pathol*. 2011;6:425–56.